Dielectric continuum model and Fröhlich interaction in superlattices

Kun Huang
Institute of Semiconductors, Chinese Academy of Sciences, P.O. Box 912, Beijing 100083, China

Bangfen Zhu*
Center of Theoretical Physics, Chinese Center of Advanced Science and Technology (World Laboratory), Beijing, China and Institute of Semiconductors, Chinese Academy of Sciences, P.O. Box 912, Beijing 100083, China
(Received 21 June 1988)

In an attempt to establish an equivalent of the Fröhlich interaction in superlattices, we are led to a critical examination of the dielectric continuum model by comparing with a parallel microscopic model. The reason that the usually quoted confined bulklike phonon modes derived from the dielectric continuum model are completely at variance with the results calculated from the microscopic model is explained. Simple rules for obtaining the proper bulklike modes are then set up, which lead to analytical expressions for the modes, which are found to agree closely with numerical results calculated from the microscopic model in the limit of zero dispersion for the bulk LO and TO phonons. They directly furnish expressions for the interaction with charged particles, which can be considered the equivalent to the Fröhlich interaction in superlattices. Phonon dispersion has the effect of mixing the interface modes into the bulklike modes with nearby frequencies. The small number of bulklike modes so affected are no longer confined to one material. The potentials of these modes apparently cannot be described by simple analytical expressions.

I. INTRODUCTION

In recent years, there have been many investigations on electronic properties of quasi-two-dimensional (2D) systems (ionic slabs, quantum wells, and superlattices),[1-4] which depend essentially on the polar interaction between electrons and optical phonons. In these works, the usual Fröhlich interaction[5] for bulk materials was used. In fact, of course, the optic vibration modes in slabs, quantum wells, and superlattices are markedly different from the modes in bulk materials.[6-10] The situation calls for an appropriate formulation of the polar interaction in such systems.

This might seem to be a problem already solved, for the usual Fröhlich interaction was derived straightforwardly by treating the lattice dynamics on the basis of the dielectric continuum model,[5,11] and such treatments of optic-phonon modes in quasi-2D systems have been in existence for many years.[6,10,12,13] Riddoch and Ridley[14] had in fact already made calculations of electron scattering in quantum wells on the basis of optic modes derived by Fuchs and Kliewer[6] on the dielectric continuum model.

However, there were indications that the node structure of the usually quoted bulklike modes derived from the dielectric continuum model disagreed with results calculated from microscopic models.[15] Strictly speaking, the dielectric continuum model is a macroscopic model which corresponds to the long-wavelength limit of the optic vibrations. Its application to systems containing sharp discontinuities like the superlattices is certainly stretching it beyond its legitimate limit. With the purpose of critically examining the continuum model as applied to superlattices, we have devised a simple microscopic model which can be considered a close microscopic counterpart of the dielectric continuum model. On the basis of results calculated from this microscopic model, we have already in an earlier paper briefly reported on certain points of doubt relating to the bulklike modes derived from the dielectric continuum model.[16]

In the following we shall present more fully the discrepancy between the bulklike modes as usually derived from the dielectric continuum model and the modes calculated from our microscopic model. This discrepancy is a manifestation of an arbitrariness in the solutions originating from certain basic limitations of the dielectric continuum model. Actually, the model in itself cannot lead to unambiguous solutions for the bulklike modes. It will be shown how simple rules can be set up, leading to analytical expressions for the bulklike modes, which show close agreement with numerical results calculated from the microscopic model. The potential associated with the bulklike modes thus obtained and the interface modes derived directly from the dielectric continuum model can be considered as providing the analogue of the Fröhlich interaction in superlattices.

In superlattices, the finite dispersion of the bulk LO and TO phonons has certain specific effects, which find no parallel in bulk materials. Thus in the presence of such phonon dispersion, a partial mixing of the interface modes into bulklike modes occurs. In the last section, such effects of phonon dispersion will be discussed.

II. MICROSCOPIC MODEL

For the purpose of investigating specifically the limitation of the dielectric continuum model owing to its mac-

roscopic nature, we have introduced a simple microscopic model, which closely parallels the dielectric continuum model.[16] An important feature of the model is that it takes proper account of the long-range Coulomb interaction and yet permits easy solution. Basically, we simulate the optic vibrations between the oppositely charged lattice particles by a simple-cubic lattice of charged oscillators. In modeling a superlattice constituted of two materials A and B, we assume that they differ only in a change in their restoring force constant. As shown in our earlier paper, this difference can be treated as a "perturbation" (not implying it being small), with the eigenmodes of the simple A lattice used as the basic vectors to express the dynamical matrix of the superlattice.

The vibrational modes of the simple A lattice normalized to the region of $N\times N\times N$ sites can be written in the form

$$\mathbf{u}(l|\mathbf{k},j)=N^{-3/2}\exp[i\mathbf{k}\cdot\mathbf{x}(l)]\mathbf{e}(\mathbf{k},j)\quad (j=1,2,3)\ , \tag{1}$$

where l labels the lattice sites located at $\mathbf{x}(l)$, $\mathbf{k}$ is the wave-number vector of the mode, and j labels the three modes for a given $\mathbf{k}$ polarized, respectively, along $\mathbf{e}(\mathbf{k},j)$. The superlattice only couples together A modes with wave vectors connected by the reciprocal-lattice vectors of the superlattice. For the sake of simplicity, we shall see our $ABAB\ldots$ superlattice as formed by m layers of A oscillators followed by m layers of B oscillators in a periodic sequence along z axis. Thus the A modes that are coupled will have wave vectors given by

$$\mathbf{k}_s=\mathbf{k}+(s\pi/ma)\hat{\mathbf{z}}\ , \tag{2}$$

where

$$s=-m,-(m-1),\ldots,0,\ldots,(m-1)\ . \tag{3}$$

$\mathbf{k}$ in (2) is now a wave-number vector appropriate to the superlattice with k_z restricted to the minizone

$$-\pi/2ma<k_z\le\pi/2ma\ . \tag{4}$$

The dynamical matrix coupling these modes can be readily worked out, namely,

$$\langle\mathbf{k}_{s'},j'|H|\mathbf{k}_s,j\rangle=\delta_{ss'}\delta_{jj'}[\omega^2(\mathbf{k}_s,j)+0.5\Delta\omega_0^2]+\left[\frac{\sin(s-s')\pi/2}{\sin(s-s')\pi/2m}\right]\frac{\Delta\omega_0^2}{2m}\times\mathbf{e}(\mathbf{k}_{s'},j')\cdot\mathbf{e}(\mathbf{k}_s,j)(1-\delta_{ss'})\ , \tag{5}$$

where $\omega^2(\mathbf{k}_s,j)$ are the squared frequencies of the A modes and $\Delta\omega_0^2$ represents the additional restoring force constant for the B oscillators expressed as a shift of the squared oscillator frequency.

The input for calculation with the microscopic model consists of the frequencies $\omega^2(\mathbf{k},j)$ and polarization vector $\mathbf{e}(\mathbf{k},j)$ for the A modes and $\Delta\omega_0^2$. In the following model calculations, we shall assume the A modes for all wave vectors to resolve into one longitudinal mode and a pair of degenerate transverse modes and their frequency dispersions are parabolic.

For a given superlattice wave number $\mathbf{k}$, one obtains from the dynamical matrix (5) $6m$ vibrational modes, which will be labeled by an index $i=1,2,\ldots,6m$. They are linear superpositions of the $3\times 2m$ coupled A modes

$$\mathbf{u}(l|\mathbf{k},i)=\sum_{s,j}a_{sj}(\mathbf{k},i)\{N^{-3/2}\exp[i\mathbf{k}_s\cdot\mathbf{x}(l)]\mathbf{e}(\mathbf{k}_s,j)\}\ . \tag{6}$$

As our ultimate aim is to obtain an electron-phonon interaction analogous to the Fröhlich interaction, which is just the potential function of an electron in the electrostatic field associated with the phonon modes, we shall want the electrostatic potential associated with the normal coordinates of the vibrational modes. When the linear coefficients $a_{sj}(\mathbf{k},i)$ are so chosen that the modes as given by (6) are orthonormal,

$$\sum_l\mathbf{u}^*(l|\mathbf{k}'i')\cdot\mathbf{u}(l|\mathbf{k},i)=\delta_{\mathbf{k}\mathbf{k}'}\delta_{ii'}\ . \tag{7}$$

Corresponding normal coordinates (complex) $Q(\mathbf{k},i)$ can be introduced by the following general expansion of the oscillator displacements in terms of the normalized modes (6):[11]

$$\sqrt{M}\,\mathbf{u}(l)=\sum_{\mathbf{k},i}Q(\mathbf{k},i)\mathbf{u}(l|\mathbf{k},i)\ , \tag{8}$$

where M is the inertial mass of the oscillators. The electrostatic potential produced by the oscillator dipoles can be generally expressed as

$$V(\mathbf{x})=-q\sum_l\mathbf{u}(l)\cdot\frac{\partial}{\partial\mathbf{x}}[1/|\mathbf{x}-\mathbf{x}(l)|]\ .$$

where q is the oscillator charge. Substituting (8), one obtains

$$V(x)=-qN^{-3/2}M^{-1/2}\sum_{\mathbf{k},i}Q(\mathbf{k},i)\sum_{s,j}a_{sj}(\mathbf{k},i)\mathbf{e}(\mathbf{k}_s,j)\cdot\frac{\partial}{\partial\mathbf{x}}\left[e^{i\mathbf{k}_s\cdot\mathbf{x}}\left[\sum_l\frac{\exp\{i\mathbf{k}_s\cdot[\mathbf{x}(l)-\mathbf{x}]\}}{|\mathbf{x}(l)-\mathbf{x}|}\right]\right]\ . \tag{9}$$

The expression in the inner parentheses is a periodic function in the simple lattice, whereas for our purpose, we desire to derive a microscopically averaged potential so as to be comparable with the dielectric continuum results and also to be compatible with the idea of a Fröhlich-type interaction. Thus we express the periodic function as a Fourier expansion and retain only the constant term which is given by[11]

$$(4\pi/|\mathbf{k}_s|^2)/v_0\ , \tag{10}$$

where v_0 is the volume of a single lattice cell. Then the potential given by (9) becomes

$$V(x)=-4\pi qN^{-3/2}v_0^{-1}M^{-1/2}\sum_{\mathbf{k},i}Q(\mathbf{k},i)\left[\sum_s a_s(\mathbf{k},i)\exp(i\mathbf{k}_s\cdot\mathbf{x})/|\mathbf{k}_s|\right] . \tag{11}$$

As the transverse A modes do not contribute to the potential, we have left out the polarization index j and the coefficient a refers to the longitudinal $\mathbf{k}$ mode.

III. THE DIELECTRIC CONTINUUM MODEL

The dielectric continuum model is fully embodied in the following pair of phenomenological equations:

$$\ddot{\mathbf{w}}=b_{11}\mathbf{w}+b_{12}\mathbf{E} ,$$
$$\mathbf{P}=b_{21}\mathbf{w}+b_{22}\mathbf{E} \quad (b_{12}=b_{21}) , \tag{12}$$

where the overdots denote double time derivative and $\mathbf{w}$ is the optical displacement between the oppositely charged ions weighted by the square root of their reduced mass divided by the volume per unit ion pair. From (12) in conjunction with the equations of electrostatics, one obtains in bulk materials either irrotational solutions, which may be taken as longitudinal waves with frequency ω_{LO} given by

$$\omega_{\mathrm{LO}}^2=-b_{11}+4\pi b_{12}b_{21}/(1+4\pi b_{22}) , \tag{13}$$

or solenoidal solutions which can be taken as transverse waves with frequency ω_{TO} given by

$$\omega_{\mathrm{TO}}^2=-b_{11} . \tag{14}$$

When we deal with only electrical quantities, the model can be more simply characterized by the dielectric function, which is obtained from (12) by eliminating $\mathbf{w}$ [assuming vibrational motion to be proportional to $\exp(i\omega t)$] and can be expressed in terms of ω_{LO} and ω_{TO} as follows:

$$\epsilon(\omega)=\epsilon_\infty(\omega^2-\omega_{\mathrm{LO}}^2)/(\omega^2-\omega_{\mathrm{TO}}^2) . \tag{15}$$

ϵ_∞ is the dielectric constant due to purely electronic polarizability [i.e., $\mathbf{w}=\mathbf{0}$ in (12)] given by

$$\epsilon_\infty=1+4\pi b_{22} . \tag{16}$$

A superlattice constituted of two materials A and B will be characterized by their respective dielectric functions

$$\epsilon_A(\omega)=\epsilon_\infty(A)[\omega^2-\omega_{\mathrm{LO}}^2(A)]/[\omega^2-\omega_{\mathrm{TO}}^2(A)] \tag{17}$$

and

$$\epsilon_B(\omega)=\epsilon_\infty(B)[\omega^2-\omega_{\mathrm{LO}}^2(B)]/[\omega^2-\omega_{\mathrm{TO}}^2(B)] . \tag{18}$$

Solutions are to be sought from the equations of electrostatics,

$$\nabla\times\mathbf{E}=\mathbf{0} \tag{19}$$

and

$$\nabla\cdot\mathbf{D}=0 , \tag{20}$$

in conjunction with the dielectric functions. Equation (19) just requires that the electric field E be derivable from an electrostatic potential $V(\mathbf{x})$

$$\mathbf{E}=-\nabla V(\mathbf{x}) . \tag{21}$$

Owing to isotropy and translational symmetry in the transverse direction the solutions can be characterized by a transverse wave number $k_\parallel$ and the potential function written as

$$V(\mathbf{x})=\exp(ik_\parallel y)\Phi(z) . \tag{22}$$

The solutions obtained from the model are divided into bulklike modes and interface modes. The bulklike modes are modes strictly confined to layers of either material and vibrating with the corresponding bulk frequencies $\omega_{\mathrm{LO}}(A)$ and $\omega_{\mathrm{TO}}(A)$ or $\omega_{\mathrm{LO}}(B)$ and $\omega_{\mathrm{TO}}(B)$. We shall be primarily concerned with the LO bulklike modes, which are alone relevant to polar interaction with charged particles. The interface modes will be taken up later.

We shall next indicate how the usually quoted LO bulklike modes are derived and then render them in a form directly comparable with the interaction potential calculated from the microscopic model.

Consider the modes vibrating with the LO frequency $\omega_{\mathrm{LO}}(A)$. For such modes, in medium A, the dielectric function and hence the displacement $\mathbf{D}$ vanish. Thereby Eq. (20) is automatically satisfied, without any further restrictions on the potential function (22). The situation is otherwise in B layers. With frequency $\omega_{\mathrm{LO}}(A)$, the dielectric function $\epsilon_B(\omega)$ is nonzero, and the Eq. (20) requires that $\nabla\cdot\mathbf{E}=0$. It follows that in the B layers

$$\frac{\partial^2\Phi}{\partial z^2}=k_\parallel^2\Phi , \tag{23}$$

which has general solutions of the form

$$\Phi=A\exp(k_\parallel z)+B\exp(-k_\parallel z) . \tag{24}$$

Since $\mathbf{D}$ vanishes in A layers on both sides of a B layer, continuity of the perpendicular component D_z requires that in a B layer E_z must vanish on both boundaries. It is readily seen that thus a potential function of the form (24) must vanish identically in the layer:

$$V(\mathbf{x})=0 \quad (B \text{ layer}) . \tag{25}$$

Finally, owing to this,continuity of the transverse electric field across the A-B interfaces require that the potential function in A layer must satisfy the boundary condition that

$$E_y=-\frac{\partial}{\partial y}V(\mathbf{x})$$
$$=-ik_\parallel V(\mathbf{x})=0 . \tag{26}$$

The usually quoted LO bulklike solutions are written down in accordance with this condition as sinusoidal standing waves with nodes at the boundaries:[6,10,12,13]

$$\Phi_n(z)=\begin{cases}\cos(n\pi z/d), & n=1,3,5,\ldots\\ \sin(n\pi z/d), & n=2,4,6,\ldots\end{cases} \tag{27}$$

where d is the thickness of the confining layer and z has its origin at midpoint of the layer.

In the dielectric continuum model, such modes are separately confined to layers of one material, without any mutual coupling. However, for convenience of comparison with the microscopic model, we shall formally introduce a k_z wave number, which relates the phases of the vibrations in different layers, so that the separate confined vibrations are organized into modes extending throughout the whole superlattice, with potential functions given by

$$V(\mathbf{x})=\Phi_n(z)\exp[ik_{\parallel}y+ik_z(2ld)] , \tag{28}$$

where $l=0,1,\ldots,L-1$ labels the successive superperiods and L is the total number of such periods, thus

$$L(2m)=N . \tag{29}$$

Both to facilitate comparison with the microscopic model and to render the results essentially in the form of an electron-phonon interaction analogous to the Fröhlich interaction, we shall want to introduce the corresponding normal coordinates and derive the potential function associated with the normal coordinates. For this purpose, we shall need the optic displacement $\mathbf{w}(\mathbf{x})$ of the vibration modes and normalize it.

For the LO bulklike modes, we have everywhere $\mathbf{D}=\mathbf{0}$, or $\mathbf{P}=-\mathbf{E}/4\pi$; the latter substituted in the second phenomenological Eq. (12) gives

$$\mathbf{w}=-(1+4\pi b_{22})\mathbf{E}/(4\pi b_{12}) , \tag{30}$$

showing that $\mathbf{w}$ is simply proportional to the electric field. With the potential functions of the vibration modes as given by (28), the corresponding optic displacement can thus be expressed as follows:

$$\begin{aligned}\mathbf{w}(\mathbf{x}|\mathbf{k},n)&=C(-\nabla V(\mathbf{x}))\\&=C(0,-ik_{\parallel}\Phi_n,-\partial\Phi_n/\partial z)\\&\quad\times\exp[ik_{\parallel}y+ik_z(2ld)] ,\end{aligned} \tag{31}$$

where C is a constant depending on normalization. Imposing the orthonormal condition

$$\int \mathbf{w}^*(\mathbf{x}|\mathbf{k}',n')\cdot\mathbf{w}(\mathbf{x}|\mathbf{k},n)d\mathbf{x}=\delta_{\mathbf{k}\mathbf{k}'}\delta_{nn'} , \tag{32}$$

the normalization constant C is readily determined and one obtains the normalized optic displacement in the following form:

$$\begin{aligned}\mathbf{w}(\mathbf{x}|\mathbf{k},n)&=N^{-3/2}V_0^{-1}I_n^{-1/2}(0,-ik_{\parallel}\Phi_n,-\partial\Phi_n/\partial z)\\&\quad\times\exp[ik_{\parallel}y+ik_z(2ld)] ,\end{aligned} \tag{33}$$

where

$$I_n=\frac{1}{2d}\int\left[k_{\parallel}^2\Phi_n^2(z)+\left(\frac{\partial\Phi_n}{\partial z}\right)^2\right]dz . \tag{34}$$

The corresponding normal coordinates $Q(\mathbf{k},n)$ are introduced by expanding general optic displacements in terms of the normalized mode displacements (33):

$$\mathbf{w}(\mathbf{x})=\sum_{\mathbf{k},n}Q(\mathbf{k},n)\mathbf{w}(\mathbf{x}|\mathbf{k},n) . \tag{35}$$

In accordance with Eq. (30), we can obtain the associated electric field by multiplying (35) with

$$-4\pi b_{12}/(1+4\pi b_{22})=-[4\pi(\omega_{\mathrm{LO}}^2-\omega_{\mathrm{TO}}^2)/\epsilon_\infty]^{1/2} . \tag{36}$$

From this field, with the explicit expression (33) for $\mathbf{w}(\mathbf{x}|\mathbf{k},n)$ substituted, one readily obtains the corresponding potential function

$$\begin{aligned}V(\mathbf{x})=&-(N^{3/2}v_0)^{-1}[4\pi(\omega_{\mathrm{LO}}^2-\omega_{\mathrm{TO}}^2)/\epsilon_\infty]^{1/2}\\&\times\sum_{\mathbf{k},n}Q(\mathbf{k},n)\{I_n^{-1/2}\Phi_n(z)\\&\times\exp[ik_{\parallel}y+ik_z(2ld)]\} .\end{aligned} \tag{37}$$

IV. THE VANISHING-PHONON-DISPERSION LIMIT AND ANALOG OF FRÖHLICH INTERACTION

In this section, we shall make calculations with the microscopic model, using parameters representing practically zero dispersion for the bulk LO and TO phonons, so as to keep the model as close as possible to the dielectric continuum model. We shall compare the mode potential calculated from (33) and (11), respectively, for the dielectric continuum model and the microscopic model. When the parameters of the two models are properly correlated, we find that the prefactors in these formulas are in fact equal. In the following comparison, this common prefactor will be left out, so actually compared are the coefficients of the Q coordinates included in brackets in (37) and (11), namely

$$I_n^{-1/2}\Phi_n(z)\exp[ik_{\parallel}y+ik_z(2ld)] \quad\text{(continuum model)} , \tag{38}$$

and

$$\sum_s a_s(\mathbf{k}\,|\,i)\exp(i\mathbf{k}_s\cdot\mathbf{x})/|\,\mathbf{k}_s\,| \quad\text{(microscopic model)} \tag{39}$$

(both have the dimension of k^{-1} and will be given in units of d/π). The mode potentials in the continuum model are clearly independent of k_z, apart from a constant phase factor (within a superperiod). The same is found to be true with the potentials calculated from the microscopic model in the limit of zero dispersion.

In Fig. 1 are compared the mode potentials calculated from the two models for a typical case ($k_{\parallel}=0.5\pi/d$). Here as well as in the following, all calculations with the microscopic model represented in the figures are made for superlattice with $m=14$. The only other relevant material parameter in the calculation with the microscopic model is

$$(\omega_{\mathrm{LO}}^2-\omega_{\mathrm{TO}}^2)/\Delta\omega_0^2$$

which hardly affects the result so long as it is appreciably smaller than 1 so that the LO-TO gaps of the two materials are well separated.

On first sight, the results from the two models seem to show a measure of agreement. But closer inspection

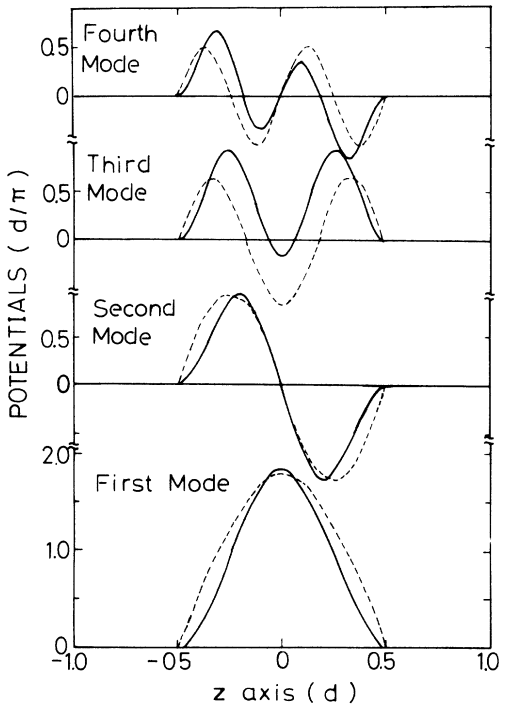

FIG. 1. Comparison of potentials of LO-confined bulklike modes [Eq. (2), dashed lines] with potentials calculated from microscopic model (solid lines) for $k_{\parallel}=0.5\pi/d$. [The material parameter $(\omega_{\rm LO}^2-\omega_{\rm TO}^2)/\Delta\omega_0^2=0.18$.]

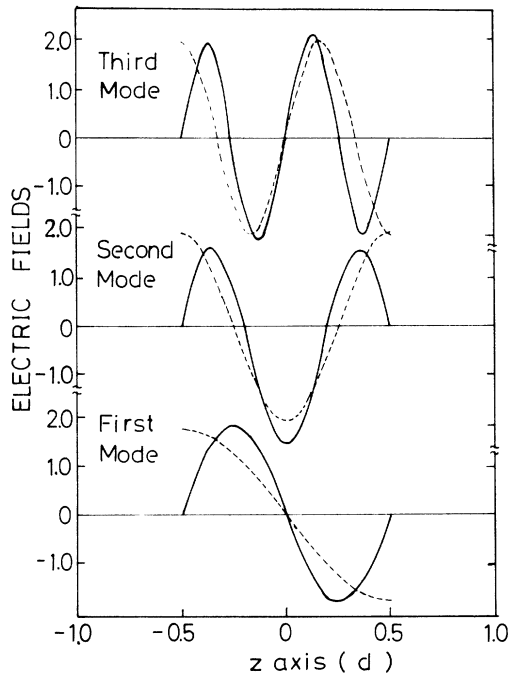

FIG. 2. Similar comparisons of electric fields along z axis as in Fig. 1.

shows radical differences. Thus the potential curves calculated from the microscopic model approach zero slopes at the interfaces located at $z=\pm d/2$, whereas the potential curves calculated from the continuum model have maximum slopes at the interfaces. In other words, the electric field has nodes at the interfaces according to the microscopic model, whereas the continuum model leads to maximum electric field at the interfaces. This difference is shown more conspicuously in Fig. 2, where the electric fields along the z axis are compared.

Figure 2 reveals yet another basic difference. It is clearly observable from the figure that the sequence of the confined modes $n=1,2,3,\ldots$ from the continuum model contains, respectively, $\frac{1}{2},1,\frac{3}{2},\ldots$ wavelengths, whereas the corresponding sequence of modes from the microscopic model contains $1,\frac{3}{2},\ldots$ wavelengths. This difference actually bears out a very significant point. Namely, judging by the usual sequence of standing waves limited to a confined length, one might say that the microscopic model appears to have lost its half-wavelength mode. This is in fact how it should be. As pointed in our earlier paper,[16] when the wave vector $\mathbf{k}$ changes from strictly along the z axis to other directions, the half-wavelength mode (referred to as "zero-node mode" in our earlier paper) changes its confined character and becomes an interface mode. In other words, for the case illustrated in Figs. 1 and 2, namely $k_{\parallel}=0.5\pi/d$, the half-wavelength mode derived from the continuum model actually should not be there.

The discontinuous drop of the electric field from its maximum to zero at the interfaces, which follows directly from the continuum-model solutions (27), is clearly unrealistic. To arrive at such results with the continuum model is not altogether surprising when we consider the following two basic limitations of the model.

(1) Owing to the neglect of phonon dispersion, all LO-confined modes are completely degenerate and any of their linear combinations can be taken as modes of the system. In this sense, the sinusoidal modes (27) are arbitrarily postulated.

(2) As a continuum model, it permits all wavelengths including infinitely short wavelengths.

Considering these limitations, the apparent ordering of the sinusoidal solutions in accordance with decreasing wavelengths in (27) is largely illusory, for these modes contain discontinuities in the field $\mathbf{E}$ and optical displacements $\mathbf{w}$ at the interfaces; this means that despite their simple appearance, actually these modes involve contents of infinitely short waves. Such a situation can arise clearly because in the continuum model such short waves are not only allowed, but also conceived as realizable with the same frequencies as the long-wavelength modes.

The above-mentioned arbitrariness is inherent in the continuum model. The dielectric continuum model by itself apparently cannot provide a useful criterion for determining the realistic bulklike modes. However, we have found that following certain clues indicated by the modes calculated from the microscopic model, we obtain simple analytical expressions for the bulklike modes showing close agreement with results calculated from the microscopic model. These clues are as follows.

(1) As clearly seen in Figs. 1 and 2, not only the potential functions calculated from the microscopic model but

also their derivatives tend to zero at the interfaces. This is of course how it should be, for only thus the modes confined to A layers can connect smoothly to B layers where both the potential and field vanish identically.

(2) Clearly a single sinusoidal solution like the usually quoted solution given in (27) cannot meet the requirement of both vanishing potential and field at the interfaces. A close look at the potential curves calculated from the microscopic model in Fig. 1. indicates that the requirement is met by certain simple composite functions. Namely, the symmetric modes are composed of a cosine function plus a constant and the antisymmetric modes are composed of a sine function plus in a simple linear term.

Following these clues, we write down for the symmetric modes

$$\Phi_n(z)=\cos[n\pi z/(m+1)a]-(-1)^{n/2}, \quad n=2,4,\ldots \tag{40}$$

where we have taken account of the fact that the potential and its derivative calculated from the microscopic model vanish close to

$$z=\pm(m+1)a/2 . \tag{41}$$

The antisymmetric mode will have the following form:

$$\Phi_n(z)=\sin[\mu_n\pi z/(m+1)a]+C_n z/(m+1)a , \tag{42}$$

where μ_n and C_n are constants to be determined by the condition that Φ_n and its derivative both vanish at the locations (41), namely,

$$\sin(\mu_n\pi/2)=-C_n/2 , \tag{43}$$

$$\cos(\mu_n\pi/2)=-C_n/\mu_n\pi , \tag{44}$$

which requires that

$$\tan(\mu_n\pi/2)=\mu_n\pi/2 . \tag{45}$$

Equation (45) gives a series of solutions for μ_n:

$$\mu_3=2.8606, \quad \mu_5=4.918, \quad \mu_7=6.95 ,$$
$$\mu_9=8.9548, \quad \mu_{11}=10.963, \quad \ldots \tag{46}$$

which approach closer and closer to the odd integers n used to label them. The corresponding C values are given by (43):

$$C_3=1.9523, \quad C_5=-1.983, \quad C_7=1.992 ,$$
$$C_9=-1.995, \quad C_{11}=1.9964, \quad \ldots . \tag{47}$$

The symmetric modes are labeled by even integers n and the antisymmetric modes by odd integers n. The sinusoidal functions in Eqs. (40) and (42) indicate that in either case, n represents (approximately in the antisymmetric case) the number of half-wavelengths contained in the confining layer. We note that the sequence of modes obtained from this scheme starts with $n=2$. In other words, the $n=1$ case, i.e., the half-wavelength mode, is automatically excluded, in agreement with the point we have raised earlier regarding such a mode.

In Figs. 3 and 4 the potentials calculated from these re-

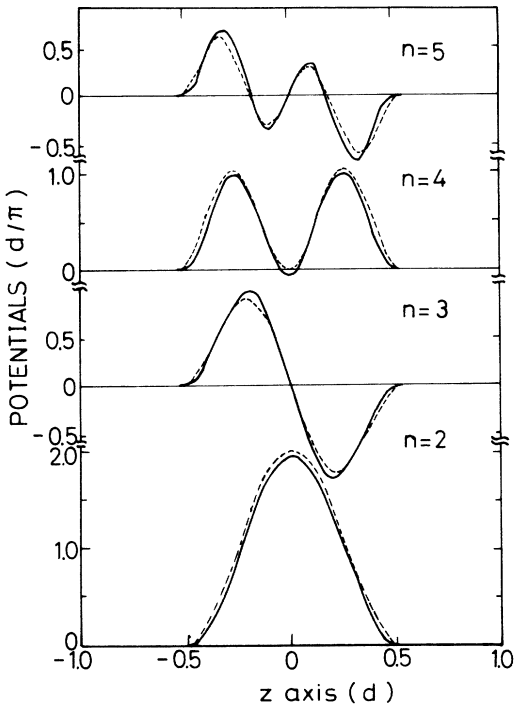

FIG. 3. Comparison of potentials of the reformulated LO-confined bulklike modes [Eqs. (40) and (42), dashed lines] with potentials calculated form microscopic model (solid lines), for $k_{\parallel}=0.1\pi/d$.

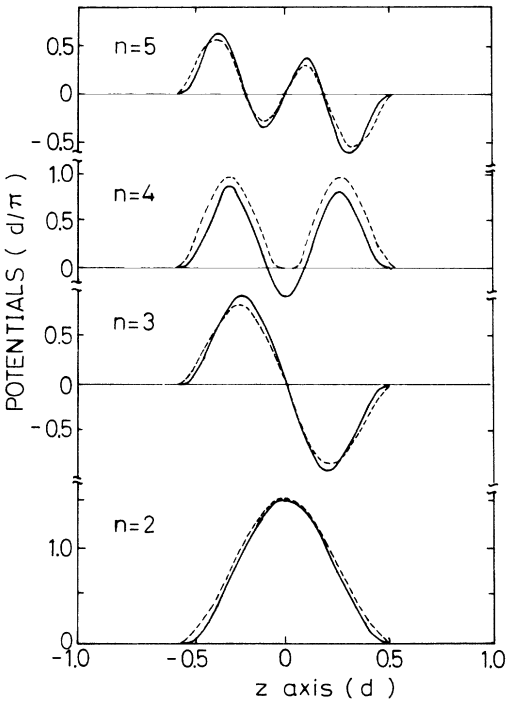

FIG. 4. Comparison of potentials of the reformulated LO-confined bulklike modes [Eqs. (40) and (42), dashed lines] with potentials calculated from microscopic model (solid lines) for $k_{\parallel}=1.0\pi/d$.

formulated modes [Eqs. (40) and (42)] are compared with potentials calculated from the microscopic model for $k_{\parallel}=0.1\pi/d$ and $1.0\pi/d$. They are seen to agree well. However, it is clearly observable that in comparison with the case of $k_{\parallel}=0.1\pi/d$ (Fig. 3), the agreement is poorer in the case of $k_{\parallel}=1.0\pi/d$ (Fig. 4). In general, we find that the agreement deteriorates with increasing $k_{\parallel}$ beyond $k_{\parallel}=1.0\pi/d$.

As we have emphasized earlier, the dielectric model imposes no restrictions whatever on the form of the potential function, apart from boundary conditions. The reformulated solutions given by (40) and (42) thus represent perfectly legitimate solutions; moreover, we have verified that the sequence of solutions $n=2,3,\ldots$ do in fact satisfy the orthogonality condition fairly closely. Therefore, the potential function $V(\mathbf{x})$ as given by (37), together with the reformulated Φ_n given by (40) and (42), can be considered as the analogue of the Fröhlich interaction in superlattices. It is, however, limited to phonon modes with $k_{\parallel}\lesssim 1.0\pi/d$. Our experience with calculations of electron scattering in quantum wells indicates that this amply covers the phonon modes relevant to electron scattering. Another limitation is the assumption of zero-phonon dispersion. This assumption of course also underlies the usual Fröhlich interaction in bulk materials. But the effect of phonon dispersion, as we shall discuss in the next section, is apparently more specific and pronounced in the case of superlattices.

The interface modes are also important for polar interaction with charged particles. But we have found that the situation with the interface modes is quite different from the bulklike modes. The interface modes are unambiguously determined by the dielectric model and, as we shall see, agree perfectly with results calculated from the microscopic model (in the zero-dispersion limit). So we shall not go into details about the derivation and normalization of the interface modes, but directly present some comparison with the results calculated from the microscopic model in Fig. 5. As before, when the parameters of the dipole lattice are properly correlated with the dielectric continuum model, the same common prefactor occurs and can be left out in the comparison. For the comparison, for both models, the relevant material parameter is $(\omega_{\mathrm{LO}}^2-\omega_{\mathrm{TO}}^2)/\Delta\omega_0^2$, which is taken to be the same (0.18) in both models. The interface modes have, in general, complex amplitudes. In Fig. 5, the calculated moduli of the potential function are represented by crosses and dots, respectively, for the continuum model and the microscopic model. The results calculated from the two models are seen to agree almost perfectly, apparently irrespective of the wave vector $\mathbf{k}$.

V. EFFECT OF FINITE DISPERSION

The vibration modes derived from the dielectric-continuum model are sharply divided into strictly confined bulklike modes and extended interface modes. Calculations with the microscopic model show that this is only true in the limit of zero dispersion for the bulk TO and LO phonons. When finite phonon dispersion is taken into account, the interface modes are partially mixed

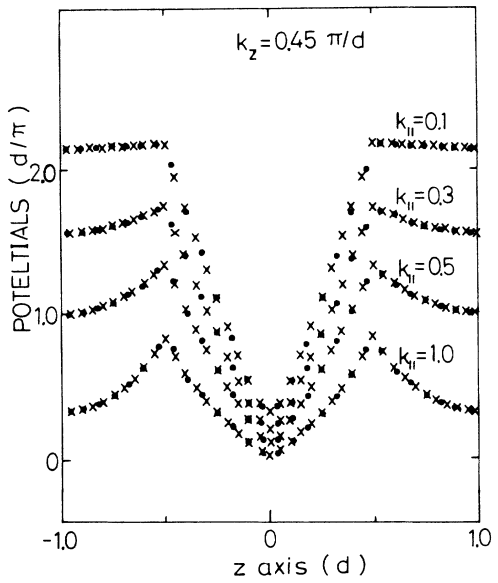

FIG. 5. Comparison of potentials (modulus) of interface modes as calculated from the continuum model (crosses) and from the microscopic model (dots). The relevant parameter $(\omega_{\mathrm{LO}}^2-\omega_{\mathrm{TO}}^2)/\Delta\omega_0^2+0.18$.

with the bulklike modes with nearby frequencies.

The interface modes calculated from the continuum model have frequencies within the $\omega_{\mathrm{LO}}-\omega_{\mathrm{TO}}$ gap of either one of the materials. Figure 6 maps out the dispersion of the interface modes within the $\omega_{\mathrm{LO}}-\omega_{\mathrm{TO}}$ gap of one material. The frequency is given as a function of the transverse wave number $k_{\parallel}$ for a number of k_z values. It is seen that for a given wave vector $(0,k_{\parallel},k_z)$, generally there are two modes with frequencies above and below the horizontal line representing the common frequency of the modes with $k_z=0$. The figure shows that with increasing k_z and decreasing $k_{\parallel}$, the upper mode will go up in frequency towards ω_{LO} and interact more strongly with the LO bulklike modes. This is shown quantitatively by the results listed in Table I, which are calculated

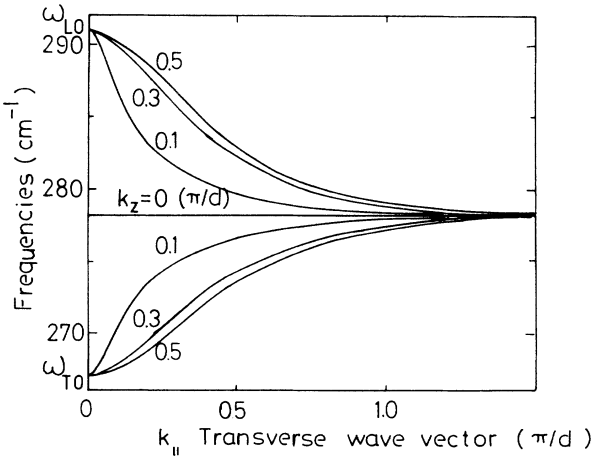

FIG. 6. Dispersion of the interface modes (continuum model).

TABLE I. Intermixing between bulklike and interface modes. For each wave number specified on the left, the figures in the first row are the mode frequencies, expressed in cm^{-1}, and the figures in the second row express the percentage of admixture of the interface mode.

Wave number (in π/d)		Mode frequency and percentage of admixture of interface mode				
$k_\parallel$	k_z	$n=2$	$n=3$	$n=4$	$n=5$	Interface mode
1.0	0.1	290.17	289.14	287.60	285.73	276.81
		0.03	0.20	0.23	1.12	42.42
	0.3	290.17	289.15	287.59	285.74	277.16
		0.01	0.31	0.07	1.76	51.77
	0.5	290.17	289.15	287.59	285.75	277.42
		0.00	0.36	0.00	2.04	64.95
0.5	0.1	290.18	289.22	287.57	285.79	278.72
		0.02	0.21	0.13	1.32	62.00
	0.3	290.18	289.23	287.57	285.88	282.07
		0.00	0.51	0.07	4.26	59.20
	0.5	290.17	289.24	287.56	285.94	282.66
		0.00	0.07	0.00	6.70	67.83
0.3	0.1	290.15	289.24	287.54	285.83	281.62
		0.01	0.30	0.08	2.38	54.96
	0.3	290.15	289.28	287.54	286.31	284.52
		0.00	1.64	0.14	30.99	58.16
	0.5	290.15	289.31	287.53	284.98	286.78
		0.00	3.06	0.00	35.61	54.30
0.1	0.1	290.13	289.31	287.52	285.18	286.92
		0.00	3.13	0.28	27.83	63.52
	0.3	290.13	288.89	287.51	285.50	290.02
		0.18	26.23	0.00	3.50	65.60
	0.5	290.13	288.95	287.52	285.51	290.25
		0.00	18.57	0.00	4.16	73.92

from the microscopic model, assuming parabolic phonon dispersions with the bandwidths of GaAs.

The table lists the first four LO bulklike modes and the upper interface mode calculated for a series of wave numbers. For each wave number specified on the left, the figures in the first row are the mode frequencies, expressed in wave-number units. The figures in the second row for each wave number express the percentage of admixture of the interface mode. This percentage is calculated from the square of the projection of the normalized mode vector on the normalized mode vector of the interface mode calculated in the zero-phonon-dispersion limit. We notice that going down the table along increasing k_z and decreasing $k_\parallel$, the interface mode goes up in frequency. In the upper half of the table, the interface mode remains some way below the bulklike modes listed, and we see that only the lowest of the latter has an appreciable admixture of the interface mode. In the last few rows, the interface mode gets right into the frequency range of the bulklike modes listed and one finds that the closest antisymmetric bulklike mode is strongly perturbed with very considerable admixture of the interface mode. The number n specifying the bulklike modes follows the convention of the preceding section; the even modes are seen to be very little affected by the interface mode owing to symmetry reasons.

In Figs. 7 and 8 are shown two examples of the LO

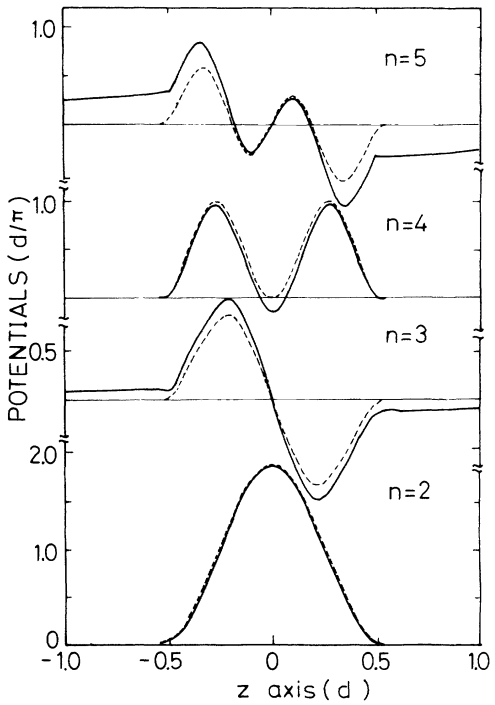

FIG. 7. LO bulklike modes calculated from microscopic model with finite phonon dispersions (solid lines) compared with reformulated modes [Eqs. (40) and (42)] for continuum model (dashed lines), for $k_\parallel = k_z = 0.5\pi/d$.

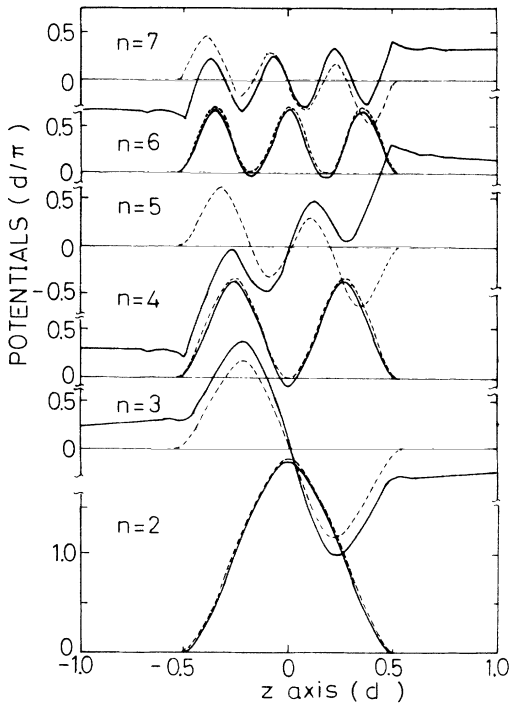

FIG. 8. LO bulklike modes calculated from microscopic model with finite phonon dispersion (solid lines) compared with the reformulated modes [Eqs. (40) and (42)] for the continuum model (dashed lines), for $k_{\parallel}=0.3\pi/d$ and $k_z=0.5\pi/d$.

bulklike modes calculated from the microscopic model with phonon dispersion taken into account (with LO and TO bandwidths taken from GaAs). Represented in this figure are the calculated mode potentials as compared with the reformulated modes of the preceding section drawn in dashed lines. In the case of $k_{\parallel}=0.5\pi/d$ and $k_z=0.5\pi/d$ represented in Fig. 7, the interface mode frequency is still some way below the bulklike modes illustrated, and only the $n=5$ mode shows conspicuous departure from the simple reformulated modes, clearly owing to the admixture of the interface mode (see Table I). In the case represented in Fig. 8, the interface mode comes between the odd modes $n=3$ and $n=5$, and we see that the $n=5$ mode is very strongly modified. The $n=3$ and $n=7$ modes, although only admixed with ~ 3–4% of the interface mode (see Table I), also show very appreciable modification, especially in the $n=7$ case. The reason is that the interface modes involve longer-wavelength components and are hence associated with stronger Coulomb potentials. So the presence of a small percentage of the interface modes may cause significant change in the mode potential, especially in the case of the higher-order modes, which are associated with proportionally lower mode potentials. The $n=7$ case is a typical example.

VI. CONCLUSIONS

In an attempt to establish an equivalent of the Fröhlich interaction in superlattices, we have been led to a critical examination of the dielectric continuum model by comparing with a closely parallel microscopic model. So long as the microscopic model also ignores the dispersion of the bulk LO and TO phonons (as in the continuum model), we find that the interface modes calculated from both models agree completely. But the usually quoted bulklike modes, supposedly derived from the dielectric continuum model, are found to be completely at variance with the modes calculated from the microscopic model. This discrepancy is due to certain arbitrariness and limitation inherent in the continuum model and realistic bulklike modes clearly cannot be determined from the model by itself. We have shown how, following certain clues provided by the modes calculated from the microscopic model, we obtain simple analytical expressions for the LO bulklike modes which agree closely with the modes calculated from the microscopic model ignoring bulk phonon dispersion.

Throughout the paper we have been careful to work with the electrostatic potential associated with properly normalized modes. In this way, in obtaining the above LO bulklike modes, we have in effect obtained an analogue of the Fröhlich interaction in superlattices.

Although bulk phonon dispersion is likewise ignored in the usual bulk Fröhlich interaction, the effect of phonon dispersion is more specific and pronounced in the case of superlattices. The effect of finite phonon dispersion is found to be mainly through the partial intermixing of the interface modes into bulklike modes with nearby frequencies. Apart from the small number of bulklike modes neighboring on the interface modes, the bulklike mode potentials as derived above remain essentially unperturbed. But in the case of the bulklike modes interacting with the interface modes, even with an admixture of a few percent of the interface modes, the mode potentials can show significant modifications, and the modes are not longer strictly confined to layers of one material.

ACKNOWLEDGMENT

This work is supported by the China National Natural Science Foundation.

*Also at the Department of Physics and Measurement Technology, Linköping University, Linköping, Sweden.

[1]K. Hess, Appl. Phys. Lett. **35**, 484 (1979).
[2]P. J. Price, Ann. Phys. (N.Y.) **133**, 217 (1981).
[3]F. A. Riddoch and B. K. Ridley, J. Phys. C **16**, 6971 (1983).
[4]S. Das Sarma and B. A. Masen, Ann. Phys. (N.Y.) **163**, 78 (1985).
[5]H. Fröhlich, Adv. Phys. **3**, 325 (1954).
[6]R. Fuchs and K. L. Kliewer, Phys. Rev. B **140**, A2076 (1965).
[7]W. E. Jones and R. Fuchs, Phys. Rev. B **4**, 3581 (1971).
[8]G. Kanellis, J. F. Morhange, and M. Balkanski, Phys. Rev. B **28**, 3406 (1983).

[9]S. K. Yip and Y. C. Chang, Phys. Rev. B **30**, 7037 (1984).
[10]M. V. Klein, IEEE J. Quantum Electron. **QE-22**, 1760 (1986).
[11]M. Born and K. Huang, *Dynamical Theory of Crystal Lattices* (Oxford University Press, Oxford, 1954).
[12]L. James, J. Licari, and Roger Evrard, Phys. Rev. B **15**, 2254 (1977).
[13]E. Evans and D. C. Mills, Phys. Rev. B **8**, 4004 (1973).
[14]F. A. Riddoch and B. K. Ridley, Physica B + C **134B**, 342 (1985).
[15]A. K. Sood, J. Menendez, M. Cardona, and K. Ploog, Phys. Rev. Lett. **54**, 2111 (1985).
[16]Kun Huang and Bangfen Zhu, Phys. Rev. B **38**, 2183 (1988).